Ubiquitin-assisted phase separation of dishevelled-2 promotes Wnt signalling

Vaishna Vamadevan[1,2], Neelam Chaudhary[1] and Subbareddy Maddika[1,*]

ABSTRACT

Dishvelled-2 (Dvl2) is an essential component of Wnt pathway, which controls several cell fate decisions during development, such as proliferation, survival and differentiation. Dvl2 forms higher-order protein assemblies in the cell that are critical for relaying the signal from upstream Wnt ligand–frizzled receptor binding to downstream effector β-catenin activation. However, the precise molecular nature and contribution of Dvl2 protein assemblies during Wnt signalling is unknown. Here, we show that Dvl2 forms protein condensates driven by liquid–liquid phase separation. An intrinsically disordered region (IDR) at the N-terminus is essential for Dvl2 phase separation. Importantly, we identified the HECT-E3 ligase WWP2 as an essential driver of Dvl2 phase separation *in vitro* and in cells. We demonstrated that ubiquitylation of Dvl2 through K63 linkage by WWP2 is required for formation of Dvl2 condensates. Phase-separated Dvl2 activates Wnt signaling by sequestering the components of destruction complex and thus relieving β-catenin. Together, our results reveal a ubiquitylation-dependent liquid–liquid phase separation as a new process through which Dvl2 forms condensates, which is necessary for transduction of Wnt signalling.

This article has an associated First Person interview with the first author of the paper.

KEY WORDS: Ubiquitin, Phase separation, Dishevelled, WWP2, Protein condensates, Wnt signalling

INTRODUCTION

Wnt/β-catenin signalling is an evolutionarily conserved pathway that is essential for embryonic and post embryonic development of all metazoans (Clevers, 2006; Teo et al., 2006). In the absence of Wnt ligand, levels of the transcriptional co-activator β-catenin are kept in check by a multi-protein assembly termed the destruction complex present in the cytoplasm. The destruction complex is constituted by scaffold proteins like APC and axin (herein referring to axin 1 or axin 2 unless otherwise specified), and kinases like GSK3β and CK1 (Stamos and Weis, 2013). The destruction complex employs casein kinase 1 (CK1) and GSK3β for the sequential serine/threonine phosphorylation of the highly conserved phospho-degron sequence at the N-terminus of the β-catenin, which is recognized by SCF$^{β\text{-}TRCP}$

[Skp-, cullin- and F-box-containing complex, with β-TRCP (BTRC) as the F-box component] E3-ubiquitin ligase (Aberle et al., 1997). As a result, β-catenin gets ubiquitylated and is targeted for subsequent proteosomal degradation. The signaling pathway is activated when the Wnt ligand binds to its transmembrane receptor, members of the frizzled (Fz) family, and the coreceptor LRP5 and LRP6 (LRP5/6), which leads to the formation of a Wnt–Fz–LRP5/6 complex (Cong et al., 2004; Tauriello et al., 2012). This complex will further recruit the cytoplasmic scaffold protein from the dishevelled (Dvl) family, which then mediates disassembly of the destruction complex and thereby stabilizes β-catenin. This will lead to the accumulation of β-catenin in the nucleus where it activates the transcription of target genes by associating with TCF/LEF transcription factors (Behrens et al., 1996; Molenaar et al., 1996).

Dvl is the critical player in the Wnt signalling pathway and absence of Dvl in the cell can completely abolish the pathway activation even in the presence of Wnt ligand (Gammons et al., 2016b). Dvl exists in three isoforms in mammals Dvl1, Dvl2 and Dvl3 (Lee et al., 2008). All the isoforms have a conserved domain architecture, which consists of DIX, PDZ and DEP domains and a C-terminal region (Gao and Chen, 2010). The DIX domain is considered essential for the functioning in Wnt/β-catenin signalling as it is critical for multimerization and association with axin, whereas the PDZ domain has been depicted to function in both canonical and non-canonical pathways (Kishida et al., 1999). On the other hand, the DEP domain has been implicated as essential for the both β-catenin dependent and Wnt planar cell polarity (PCP) pathway (Gammons et al., 2016b; Moriguchi et al., 1999).

The Dvl proteins have a distinct ability to form cytoplasmic puncta in cells, which is essential for functional activation of Wnt/β-catenin signalling (Schwarz-Romond et al., 2007b). Cytoplasmic puncta of endogenous Dvl have been observed in a wide variety of species with the activation of Wnt signalling (Hawkins et al., 2005; Miller et al., 1999; Torres and Nelson, 2000; Yanagawa et al., 1995). The ability of Dvl2 to form cytoplasmic puncta is often associated with its DIX-dependent polymerization (Fiedler et al., 2011; Schwarz-Romond et al., 2007a). Some recent studies using HEK293T cells in which a C-terminal GFP fusion was knocked into the endogenous Dvl2 locus claim that limited oligomerization in response to the Wnt ligand is sufficient enough to transduce the Wnt signal downstream, thus challenging the concept that higher-order assemblies of Dvl2 are necessary in cells (Kan et al., 2020; Ma et al., 2020). However, studies on the conformation of Dvl that highlight the importance of C-terminus in keeping Dvl in an appropriate autoinhibited state, calls into question the use of C-terminally tagged Dvl fusion proteins to study its function and cellular localization as they might not truly represent the wild-type Dvl because those proteins cannot be autoinhibited (Lee et al., 2015; Qi et al., 2017). Hence, the identity of Dvl puncta, their precise contribution to Wnt pathway and the molecular machineries that govern their formation remain enigmatic. Therefore, using a variety

V.V., 0000-0002-9681-2884; N.C., 0000-0002-0327-2824; S.M., 0000-0002-5880-391X

of cellular and biochemical techniques, we set out to investigate the molecular identity of Dvl2 puncta. Our study demonstrates that Dvl2 protein assemblies are phase-separated condensates that play a crucial role in the disassembly of the destruction complex to promote Wnt signalling. Additionally, we found that K63-linked ubiquitylation by WWP2 facilitates the phase separation of Dvl2.

RESULTS

Dvl2 forms liquid–liquid phase-separated protein condensates

While attempting to identify the nature of Dvl protein assemblies, and consistent with earlier studies, we observed that overexpressed Dvl2 (Fig. S1A) forms discrete small puncta-like structures early upon its expression. Interestingly, these protein assemblies grow in size over time (Fig. 1A) suggesting their dynamic nature in cells, which is reminiscent of phase-separated protein condensates. Dvl2 forms condensates in cells from different origin such as U2OS (osteosarcoma epithelial cells), HepG2 (hepatocellular carcinoma cells) and RPE1 (retinal pigment epithelial cells) cells (Fig. S1B), suggesting that this is not a cell-type-specific phenomenon. Remarkably, as time progresses these condensates change their morphology from solid to hollow or shell-like structures, which is possibly to sequester the proteins inside the condensates. Proteins with intrinsically disordered regions have the propensity to form liquid–liquid phase-separated condensates (Boeynaems et al., 2018). Indeed, analysis of Dvl2 protein sequence suggested the presence of two intrinsically disordered regions – IDR1 at the N-terminus between the DIX and PDZ domains, and IDR2 at the C-terminal region (Fig. S1C). Thus, we next tested whether Dvl2 displayed liquid-like phase-separated condensate behaviour. The fluorescence recovery after photobleaching (FRAP) signal of GFP-tagged Dvl2 (Fig. S1D) was determined (Fig. 1B,C), which suggested that the droplets had a mobile nature. In addition, two encountering Dvl2 protein droplets merged and blended into a larger sphere (Fig. 1D), indicating that Dvl2 protein assemblies in living cells are highly dynamic and possess liquid-like condensate properties. Furthermore, treatment of cells with 1,6-hexanediol (a chemical suppressor of phase separation; Elbaum-Garfinkle, 2019; Molliex et al., 2015; Ribbeck and Gorlich, 2002; Wegmann et al., 2018) followed by time-lapse analysis shown rapid loss of Dvl2 puncta in cells (Fig. 1E), thus clearly supporting our observation that Dvl2 assemblies are not mere protein aggregates but are liquid–liquid phase-separated condensates. Previously, Dvl2 has been shown to associate with endocytic machinery such as clathrin–AP2 adaptor to assist in receptor internalization and the formation of intracellular signal transducer complexes during Wnt signalling (Yu et al., 2007). In addition, recent work has suggested that liquid-like protein droplets catalyse the assembly of endocytic vesicles. However, Dvl2 did not colocalize with the early (Rab5), late (Rab7) or recycling (Rab11) endosomes (Fig. S1E), nor multi-vesicular bodies (CD63) or lysosomes (LAMP2) (Fig. S1F), possibly suggesting no involvement of endocytic pathways in the formation of Dvl2 assemblies. To understand whether the Dvl2 condensate formation is a physiologically relevant event in cells and not an overexpression-induced artefact, owing to non-availability of immunofluorescence grade Dvl2 antibodies, we established a stable cell line expressing Dvl2 at very low levels (Fig. S1G). Although these stable cells did not display Dvl2 protein condensates under normal conditions, treatment with Wnt3a readily promoted the assembly of Dvl2 condensates (Fig. 1F,G), suggesting that phase-separated condensate formation of Dvl2 is a physiologically

relevant event during Wnt signalling. Next, to understand the regions of Dvl2 that are required for condensate formation, we generated various deletion mutants of Dvl2, which lacked different domains (Fig. 1H). To avoid interference from the endogenous proteins, we expressed individual Dvl2 deletion constructs in Dvl2 knockout (KO) (Fig. S1H) HEK293T cells. Although full-length, along with PDZ deleted and CT deleted, Dvl2 could readily form liquid condensates, deletion of DIX domain, DEP domain or IDR1 regions significantly reduced the formation of condensates in cells (Fig. 1I,J). DIX and DEP domains are very well known to assist in oligomerization of Dvl2 (Gammons et al., 2016a; Kishida et al., 1999); however, deletion of IDR1 has no effect on the oligomerization of Dvl2 (Fig. S1I). Therefore, our data suggest that oligomerization of Dvl2 along with the presence of an intrinsically disorder region at the N-terminus is necessary for Dvl2 phase separation in cells.

WWP2 E3 ligase activity is required for Dvl2 phase separation

To identify the molecular machineries that control Dvl2 phase separation, we performed a Dvl2 interactome analysis in cells. By using a biochemical tandem affinity purification of a SFB-triple-tagged (streptavidin-binding protein, Flag and S-peptide) Dvl2 followed by mass spectrometry, we identified protein complexes associated with Dvl2 in cells (Fig. 2A; Table S1). Among the Dvl2-associated proteins, deletion of the E3 ligase WWP2 in cells (Fig. S2A) resulted in severe impairment of Dvl2 condensate formation (Fig. 2B). WWP2, also known as atrophin-1 interacting protein 2 (AIP2), is a HECT-type E3 ubiquitin ligase that plays an important role in cellular processes, such as transcription, translation and oncogenic signalling (Li et al., 2007; Lv et al., 2014; Maddika et al., 2011; Xu et al., 2004). Previously, WWP2 was found to be associated with Dvl2, and Dvl2 was shown to be necessary for full activation of WWP2, but the effect of WWP2 E3 ligase activity on Dvl2 was not clear (Mund et al., 2015). Importantly, we found that expression of wild-type, but not a catalytically inactive (C/A) mutant of WWP2 restored Dvl2 condensates that were lost in WWP2 KO cells (Fig. 2B,C). shRNA-mediated depletion of WWP2 in various cell lines, such as U2OS (Fig. S2B), HEPG2 (Fig. S2C) and RPE1 (Fig. S2D), also led to defective Dvl2 condensate formation (Fig. S2E–J), suggesting a cell line-independent role of WWP2 in controlling Dvl2 phase separation. Dvl2 condensate formation was specifically dependent on WWP2, as depletion of other closely related HECT E3 ligases, such as WWP1 (Fig. S3A) and NEDD4L (Fig. S3B), did not affect Dvl2 condensate formation in cells (Fig. S3C,D). Given that catalytically active WWP2 restored Dvl2 condensates in WWP2 KO cells, we next tested whether WWP2 ubiquitylated Dvl2. Firstly, we confirmed the endogenous association of WWP2 and Dvl2 in cells (Fig. 2D,E). Next, we showed that expression of wild-type but not the catalytically inactive C/A mutant of WWP2 promoted Dvl2 ubiquitylation in cells (Fig. 2F). By contrast, depletion of WWP2 led to reduced ubiquitylation of Dvl2 (Fig. S3E). Endogenous steady-state levels of Dvl2 were unaltered in WWP2-depleted cells (Fig. S3F) as well as WWP2 KO cells (Fig. S3G). No changes were observed in the half-life of Dvl2 in the presence of catalytically active WWP2 (Fig. S3H), thus suggesting that WWP2-mediated ubiquitylation on Dvl2 does not lead to its degradation. Interestingly, a ubiquitylation assay using various ubiquitin lysine to arginine mutants strongly indicated that WWP2 mediates the K63 type of ubiquitin linkage on Dvl2, as transfer of ubiquitin to the substrate failed in the presence of the ubiquitin K63R mutant (Fig. 2G). To directly test whether WWP2 mediated ubiquitylation is required for Dvl2 condensate
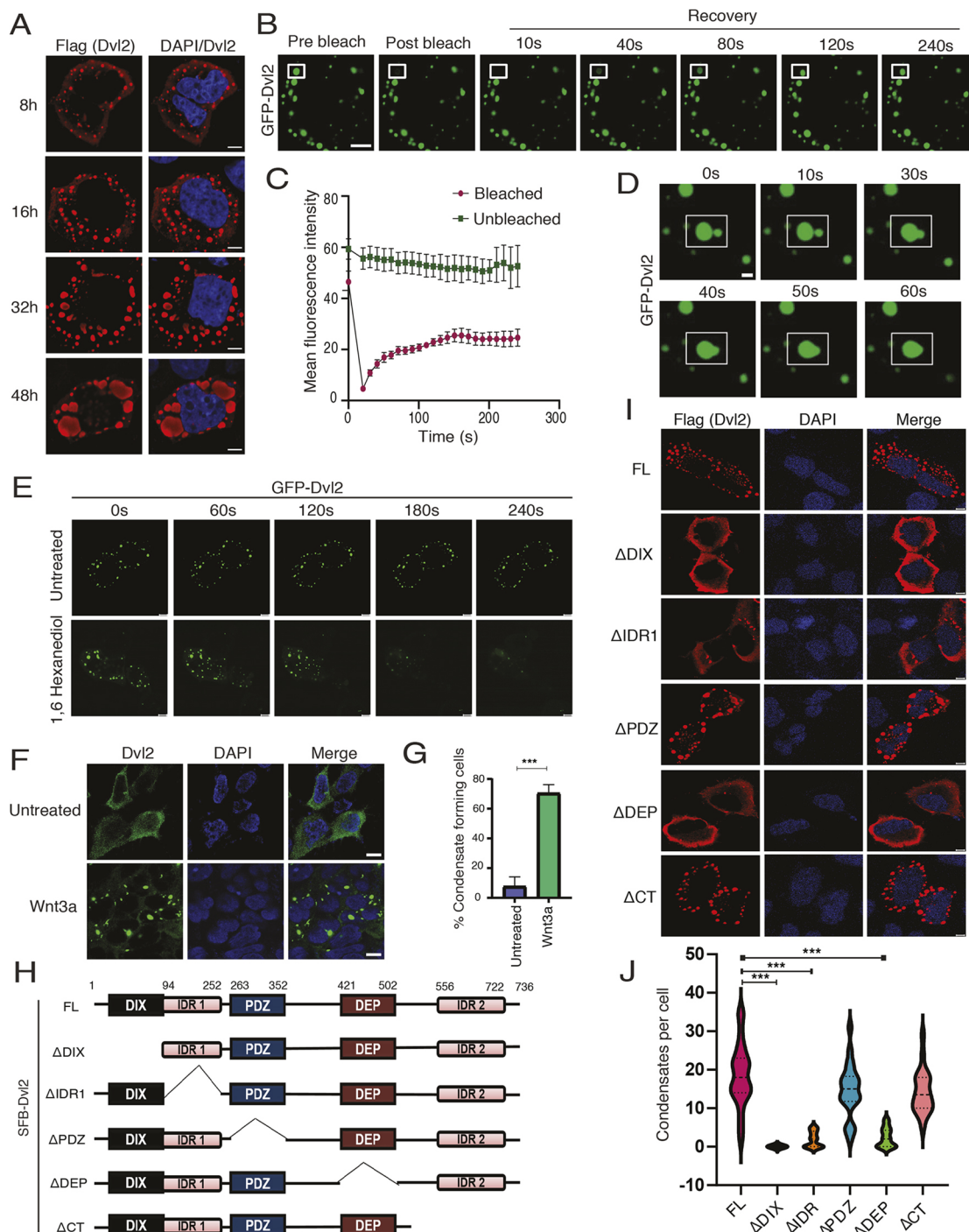
Fig. 1. Dvl2 forms liquid–liquid phase-separated protein condensates. (A) HEK293T cells transfected with SFB-tagged Dvl2. Cells were fixed at different time points after transfection and stained with anti-Flag antibody. Images were captured using a confocal microscope. DAPI is used to counterstain nucleus. Scale bars: 5 μm. (B) GFP–Dvl2-expressing cells were selectively bleached at the indicated region and the recovery was monitored by capturing images at every 10 s using a confocal microscope. Scale bar: 5 μm. (C) Graph showing the mean±s.e.m. fluorescence intensities of five independent condensates derived from bleached and unbleached areas over the indicated time course. (D) HEK293T cells expressing GFP–Dvl2 were imaged by using live-cell microscopy and the fusion of condensates was monitored over indicated times as highlighted by the boxed region. Scale bar: 1 μm. (E) Cells expressing GFP–Dvl2 were either left untreated or treated with 3% 1,6-hexanediol, and images were acquired using a live-cell imaging microscope (Leica). Scale bars: 5 μm. (F) HEK293T cells stably expressing SFB–Dvl2 at near endogenous levels were left untreated or transfected with Wnt3a. At 24 h post transfection, cells were fixed and probed with anti-Flag antibody and imaged using a confocal microscope. Scale bars: 10 μm. (G) Quantification of the percentage of cells forming condensates. mean±s.e.m., n=30 cells. ***P<0.001 (unpaired two-tailed Student's t-test). (H) Schematic representation of the full-length and various deletion mutants of SFB-tagged Dvl2 used here. Numbers on the top indicate the precise amino acid number for each domain in the full-length Dvl2 protein. (I) Dvl2 KO HEK293T cells expressing SFB-tagged full-length and different deletion mutants of Dvl2 were fixed after 24 h of transfection. Fixed cells were stained with anti-Flag antibody and imaged under a confocal microscope. Scale bars: 5 μm. (J) Quantification as violin plots of the number of condensates formed per cell expressing SFB-tagged full-length or various domain deletion mutants of Dvl2. The dashed lines represent the median and interquartile range, n=25 cells. ***P<0.0001 (one-way ANOVA with Tukey's multiple comparisons test). Images shown in A, D and E are representative of three independent experiments.
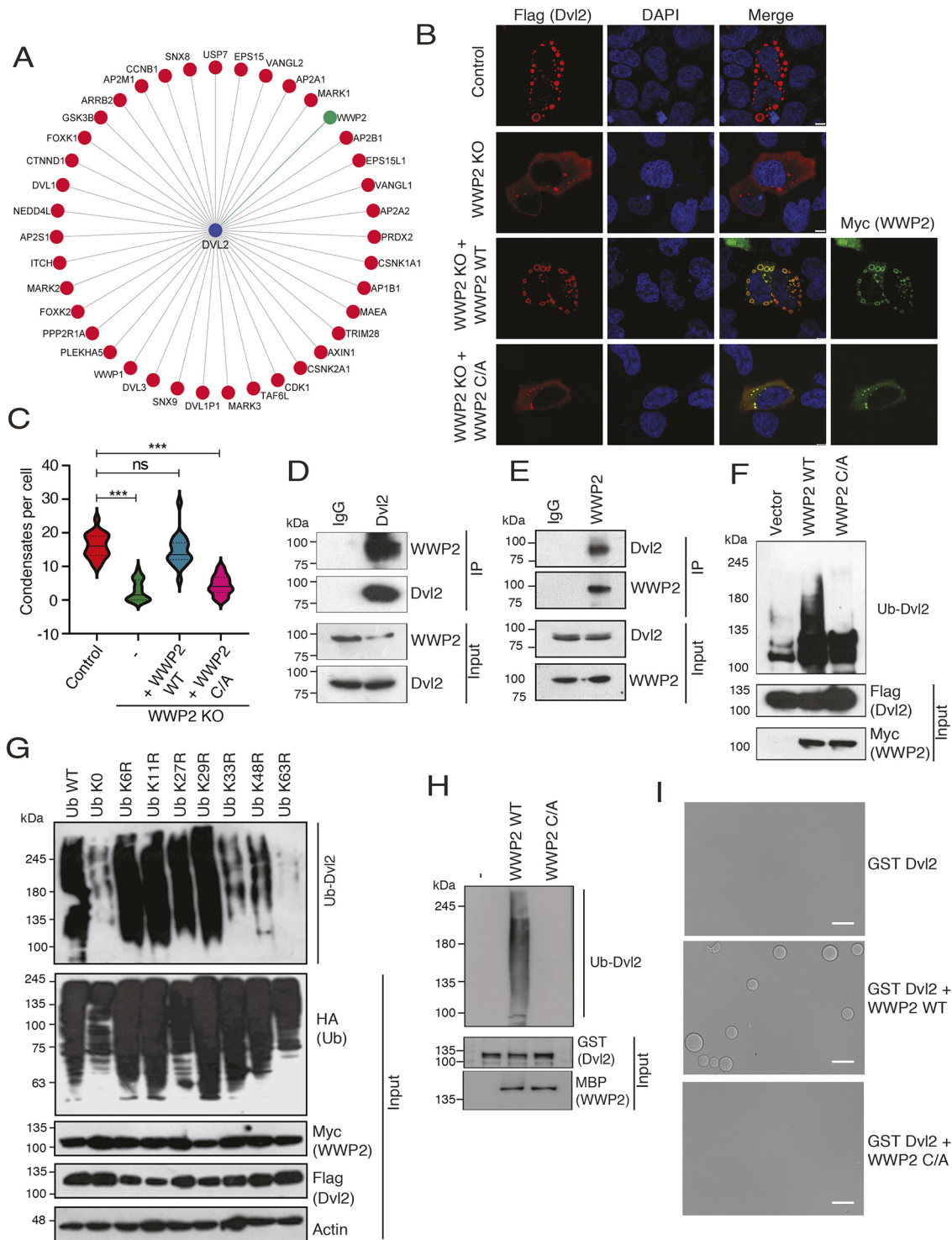
Fig. 2. See next page for legend.

formation, we employed an *in vitro* reconstitution assay to assess phase separation. The *in vitro* ubiquitylation assay using purified recombinant proteins suggested that wild-type WWP2, but not the C/A mutant, could readily ubiquitylate GST–Dvl2 (Fig. 2H). In conditions where bacterially purified recombinant GST–Dvl2 do not form condensates *in vitro*, WWP2-mediated ubiquitylation enabled Dvl2 to form phase-separated droplets (Fig. 2I). Therefore, these data support our hypothesis that WWP2-mediated ubiquitylation promotes Dvl2 phase separation.

Ubiquitylation is necessary for Dvl2 condensate formation

To further understand whether ubiquitylation is necessary for phase separation of Dvl2, we modulated the ubiquitylation machinery in cells and tested for Dvl2 condensate formation. Depletion of the E1 enzyme (UBA1), which catalyses the first step of ubiquitin conjugation, by two independent shRNAs (Fig. S4A) drastically reduced the number of Dvl2 condensates in cells (Fig. 3A,B). Subsequently, we generated recombinant fusion proteins with either the wild-type active deubiquitylase domain (DUB) or an inactive

Fig. 2. WWP2 E3 ligase activity is required for Dvl2 phase separation.
(A) Interaction network of Dvl2 with its associated proteins derived from
mass spectrometry analysis is shown. Green line indicates Dvl2 interaction
with WWP2. (B) Control and WWP2 KO cells were transfected with
SFB–Dvl2. For rescuing the phenotype, WWP2 KO cells were co-transfected
with either Myc–WWP2 wild-type (WT) or a catalytically dead mutant (C/A).
Cells were fixed and stained with anti-Flag and anti-Myc antibodies. Images
were taken using a confocal microscope. Scale bars: 5 μm.
(C) Quantification as violin plots of the number of condensates per cell for
the indicated conditions. Solid line represents the median, dashed line the
interquartile range, $n=20$. ***$P<0.001$ (one-way ANOVA with Tukey's multiple
comparisons test). (D) HEK293T cell lysates were subjected to
immunoprecipitation with either IgG or Dvl2 antibody. The presence of
WWP2 in Dvl2 immunoprecipitates was detected by western blotting with
WWP2 antibody. The presence of the protein in the lysate was detected by
loading 5% of the input. (E) HEK293T cell lysates were subjected to
immunoprecipitation with either IgG or WWP2 antibody. Presence of Dvl2 in
WWP2 immunoprecipitates was detected by western blotting with Dvl2
antibody. (F) HEK293T cells were co-transfected with SFB–Dvl2 and
Myc–WWP2 WT or the catalytically inactive mutant. At 24 h post transfection,
cells were lysed in denaturing conditions and subjected to pulldown with
streptavidin–Sepharose beads. Ubiquitylation of Dvl2 was detected by
western blotting with ubiquitin antibody. (G) SFB–Dvl2 was co-transfected with
single lysine mutants of HA-tagged ubiquitin (Ub) in the presence of WWP2.
Cells were lysed under denaturing conditions. SFB–Dvl2 was pulled down
using streptavidin–Sepharose and immunoblotted with indicated antibodies.
(H) Bacterially purified GST–Dvl2 bound to glutathione–Sepharose beads was
used as substrate for in vitro ubiquitylation with MBP WWP2 WT or the
catalytically inactive mutant. Ubiquitylation of GST–Dvl2 was detected by
immunoblotting with anti-Ub antibody. 5% input was loaded in the gel to
detect the proteins. (I) GST–Dvl2 alone or in vitro ubiquitylated Dvl2 by
WWP2 was mixed with phase separation buffer. The proteins mounted on to
a glass slide and liquid droplets formed by Dvl2 were imaged using bright field
microscope. Scale bars: 2 μm. Blots shown in D–H and images in I are
representative of three independent experiments.

C/S mutant of DUB fused at the N-terminus of Dvl2 (Fig. 3C).
Whereas Myc–Dvl2 could readily form condensates, the presence
of an active deubiquitylase domain, which cleaves ubiquitin chains,
means Dvl2 condensates fail to form in cells (Fig. 3D,E). Fusion of
a catalytically inactive DUB domain did not affect Dvl2 condensate
formation, therefore clearly suggesting that Dvl2 ubiquitylation
is essential for phase separation. Specifically, the K63 type of
ubiquitin chain linkage was necessary for Dvl2 phase separation, as
Dvl2 condensate formation was lost upon expression of Ub K63R
mutant in cells (Fig. 3F,G). As we have established that
ubiquitylation is required for Dvl2 phase separation, we next
sought to identify the sites of ubiquitylation on Dvl2 mediated by
WWP2. There are multiple lysine residues in Dvl2 protein
sequence. We mutated each of the individual lysine residues that
could potentially be ubiquitylated by WWP2 and screened for the
ability of these proteins to form phase-separated condensates.
Mutation of any single lysine residues did not affect their ability to
form condensates (Fig. S4B). Even a combination of mutants in a
cluster did not alter their ability to phase separate in cells (Fig. S4C),
possibly suggesting that multiple lysine residues located in different
domains of Dvl2 might be ubiquitylated by WWP2. In fact, this is in
agreement with a previous study that has identified multiple
ubiquitylated lysine residues on Dvl2 by using mass spectrometry
analysis (Tauriello et al., 2010). After testing various combination
of lysine mutants, we found that a protein with mutation of eight
different lysine residues (K15, K30, K44, K54, K68, K274, K301
and K343) (Fig. S4D) that were located on DIX and PDZ domains
of Dvl2 to arginines (8KR mutant) showed reduced ubiquitylation
by WWP2 (Fig. 3H). Consequent with this, the 8KR mutant was
defective in forming Dvl2 condensates (Fig. 3I,J). The failure of

8KR mutant to form condensates was not due to defects in Dvl2
oligomerization as the mutant retained its full ability to oligomerize
and interact with other Dvl2 molecules (Fig. S4E). Taken together,
these data indicate that WWP2-dependent ubiquitylation of Dvl2
via the K63 type of linkage is required for formation of protein
condensates.
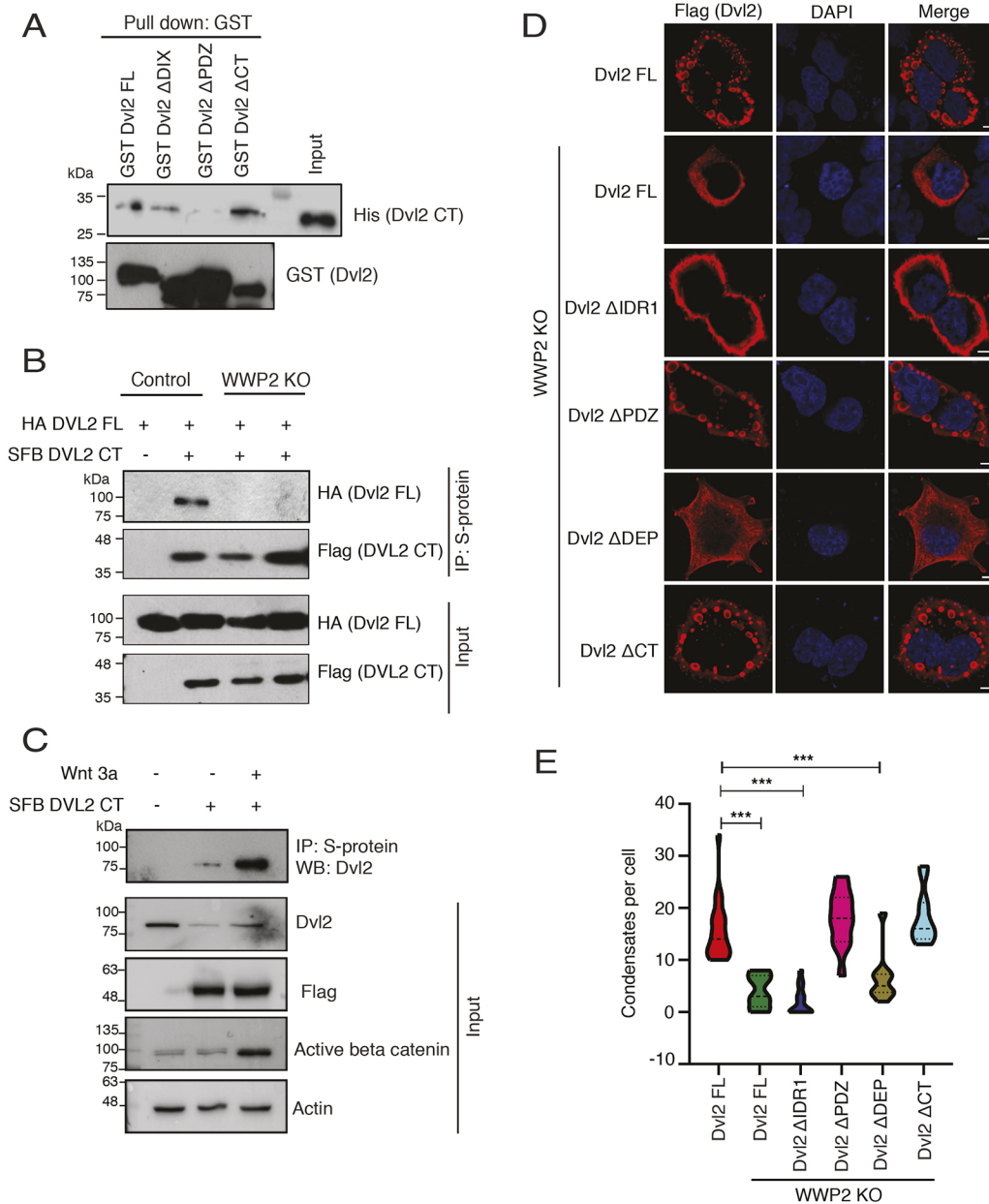
WWP2 promotes Dvl2 open configuration
Next, we sought to gain further insights of how WWP2-mediated
ubiquitylation promotes Dvl2 phase separation. Dvl is thought to
exist in open and closed conformations in cells (Lee et al., 2015;
Qi et al., 2017). The C-terminal region folds back on to the N-
terminus of Dvl and creates a closed conformation, and activation of
cells with Wnt ligands has been demonstrated to induce the open
Dvl conformation (Harnoš et al., 2019). By using bacterially
purified recombinant proteins, we confirmed that the N-terminal
PDZ domain is required for interaction with the C-terminal domain
(CT) of Dvl2 (Fig. 4A). Given that the IDR1 region, that was
necessary for Dvl2 phase separation, is located on the N-terminus
adjacent to the PDZ domain, we hypothesized that the IDR might be
hidden when the protein was in closed conformation. In addition,
because the Dvl2 ubiquitylation sites were mapped to DIX and PDZ
domains that sandwich the IDR1 region, WWP2-mediated
ubiquitylation might expose the IDR1 region for condensate
formation by switching Dvl2 into an open configuration.
Therefore, we tested the requirement of WWP2 for switching
Dvl2 from the closed to open conformation in cells by testing the
interaction of a trans-CT domain fragment with -ength Dvl2. In
control cells, the CT fragment could readily interact with full length
Dvl2 owing to its dynamic switching from the closed to the open
state. However, in WWP2 KO cells, full-length Dvl2 remains in a
constitutively closed conformation and therefore exogenous
CT fragment with no access to free N-terminus, could not interact
with full length Dvl2 (Fig. 4B). To further test whether WWP2-
dependent switching of Dvl2 conformation is a Wnt-regulated event,
we tested the interaction of CT domain with endogenous Dvl2 under
Wnt 'OFF' and 'ON' conditions. Treatment of cells with Wnt3a
readily enhanced the interaction of CT fragment with endogenous
Dvl2 (Fig. 4C), thus suggesting that Dvl2 conformational switching
is a Wnt-regulated event. If, as hypothesized, WWP2 were switching
Dvl2 from a closed to open configuration to facilitate condensate
formation, we reasoned that a constitutive open Dvl2 state might
overcome the requirement for WWP2 in condensate formation.
Indeed, whereas the full-length and IDR1-deleted version of Dvl2
were defective in condensate formation in WWP2 KO cells, mutants
with deletion of the PDZ or CT domain (constitutive open Dvl2
forms) retained the capacity to form condensates in cells even
in the absence of WWP2 (Fig. 4D,E). Thus, the constitutively
open configuration of Dvl2 (ΔPDZ and ΔCT versions) overcame the
requirement for WWP2 to form condensates in cells, clearly
suggesting that WWP2 promotes the open Dvl2 conformation, thus
exposing the IDR and thereby enabling condensate formation.

Dvl2 phase separation promotes Wnt signalling
As Dvl2 is a central component of Wnt signalling, we next
investigated the functional significance of WWP2-driven Dvl2
condensate formation in the Wnt/β-catenin pathway. We noted that
loss of WWP2 has no effect on Dvl2 association with the upstream
components of Wnt signalling pathway; Dvl2 was able to interact
with Fz receptor (Fig. S5A), CK1ε (Fig. 5B) and axin 1 (Fig. 5C) in
WWP2 KO cells as efficiently as in wild-type cells. Among many
possibilities, one of the important reasons that proteins may form
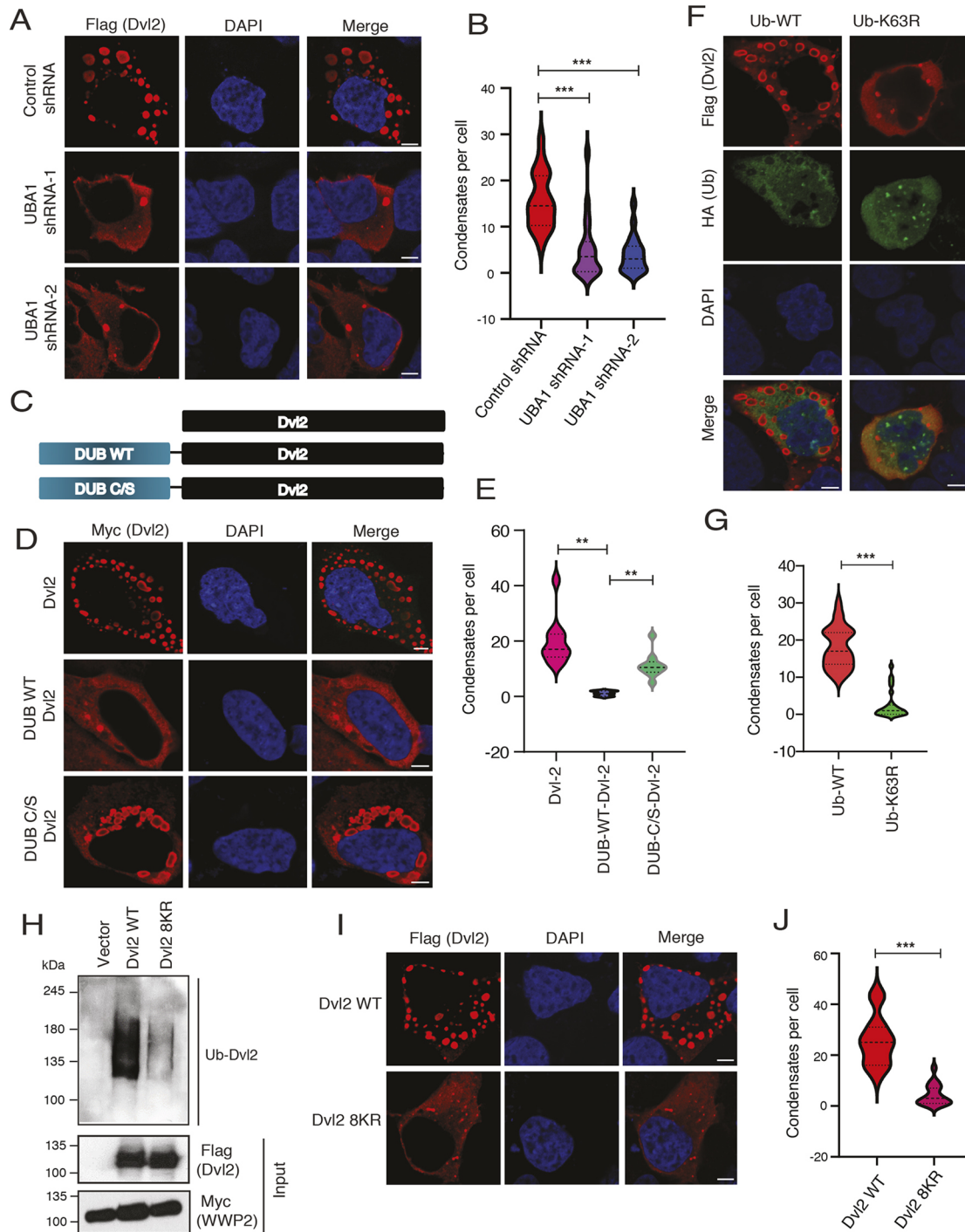
Fig. 3. Ubiquitylation is necessary for Dvl2 phase separation. (A) HEK293T cells treated with control shRNA or UBA1 shRNA for 48 h were transfected with SFB–Dvl2 for 24 h. Cells were fixed, stained with anti-Flag antibody and were imaged using a confocal microscope. Scale bars: 5 μm. (B) Quantification as violin plots of condensates formed per cell in control or UBA1 shRNA-expressing cells. n=20. ***P<0.001 (one-way ANOVA with Tukey's multiple comparisons test). (C) Schematic representation of Dvl2 fusion proteins with DUB domains (WT, wild type; C/S, catalytically inactive version). (D) HEK293T cells were transfected with a Myc-tagged full-length or WT DUB domain or catalytically inactive DUB domain fused to Dvl2 for 24 h. Cells were then fixed and stained with anti-Myc antibody and imaged under a confocal microscope. Scale bars: 5 μm. (E) Quantification of condensates formed by Dvl2 per each cell in the indicated condition was plotted. n=10. **P<0.01 (one-way ANOVA with Tukey's multiple comparisons test). (F) SFB–Dvl2 was co-transfected with HA-tagged ubiquitin (Ub) WT or K63R Ub for 24 h in HEK293T cells. Cells were fixed, stained with anti-HA and anti-Flag antibodies, and were imaged under a confocal microscope. Scale bars: 5 μm. (G) Quantification of Dvl2 condensates formed in each cell in the presence of Ub wild-type and K63R mutant was plotted. n=25. ***P<0.001 (unpaired two-tailed t-test). (H) HEK293T cells were transfected with SFB–Dvl2 WT or SFB–Dvl2 8KR mutant along with WWP2. At 24 h post transfection cells were lysed under denaturing conditions and the lysate was subjected to streptavidin–Sepharose-based pull down. Dvl2 ubiquitylation was detected by immunoblotting with anti-Ub antibody. (I) Cells expressing either SFB–Dvl2 WT or the 8KR mutant were stained with anti-Flag antibody and the condensates were imaged under a confocal microscope. Scale bars: 5 μm. (J) Quantification of condensates formed in each cell expressing WT Dvl2 or the 8KR mutant. n=20. ***P<0.001 (unpaired two-tailed t-test). The dashed lines in violin plots represent the median and interquartile range. Blot shown in H is representative of three independent experiments.

Fig. 4. WWP2 promotes Dvl2 open configuration. (A) Glutathione–Sepharose beads bound to bacterially expressed recombinant GST Dvl2 full-length or the indicated domain deletions were incubated with 7 µg of bacterially expressed recombinant His–Dvl2 C-terminal fragment (CT). Interaction of His–CT-Dvl2 with GST Dvl2 was detected by immunoblotting with anti-His antibody. (B) Control and WWP2 KO cells were co-transfected with SFB–Dvl2-CT and HA–Dvl2 full-length for 24 h. Cells were then lysed and incubated with streptavidin-Sepharose beads. Interaction between SFB–Dvl2-CT and HA–Dvl2 full-length was detected by immunoblotting with anti-HA antibody. (C) Cells transfected with SFB–Dvl2-CT were treated with either Wnt3a or left untreated. The interaction between SFB–Dvl2-CT and endogenous Dvl2 was detected by immunoblotting with Dvl2 specific antibody after immunoprecipitation with S-protein beads. Inputs in A–C are 5%. Blots shown in A–C are representative of two independent experiments. (D) Control cells were transfected with SFB–Dvl2 full-length and WWP2 KO cells were transfected with SFB–Dvl2 full-length, or SFB–Dvl2 ΔIDR1, ΔPDZ, ΔDEP or ΔCT constructs. After 24 h of transfection, cells were fixed and stained with anti-Flag antibody. Images were taken using a confocal microscope. Scale bars: 5 µm. (E) Quantification as violin plots of the number of Dvl2 condensates per cell in the indicated conditions. The dashed lines represents the median and interquartile range. n=10. ***P<0.001 (one-way ANOVA with Tukey's multiple comparisons test).

higher-order phase separated condensates is to sequester specific protein complexes in a context-dependent manner. Given that we observed that Dvl2 forms hollow condensate in cells, we reasoned that Dvl2 may be sequestering the components of destruction complex, relieving β-catenin and thereby positively promoting Wnt signalling. In accordance with our hypothesis, we found that several components of the destruction complex such as GSK3β, CK1 and axin 1, but not β-catenin, were efficiently partitioned into Dvl2 condensates (Fig. 5A,B). Sequestration of GSK3β in Dvl2 condensates was observed in multiple cell lines (Fig. S5D). This suggests that occupancy of destruction complex components gives the hollow appearance to the condensates, and it is not caused by the inaccessibility of antibody to penetrate the centre of the condensate, as previously reported (Schwarz-Romond et al., 2005). We also carried out luciferase reporter assays with the TOP FLASH reporter plasmid, which has Wnt-responsive regions upstream of the promoter that drive luciferase gene expression, to evaluate the impact of phase separation in Wnt signalling. The luciferase

experiments suggest that phase separation of Dvl2 is necessary for Wnt activation, as deletion of the IDR1 region (Fig. S5E) severely compromised the ability of Dvl2 to enhance the activity of Wnt-responsive promoters (Fig. 5C). Likewise, expression of the ubiquitin K63R mutant, which leads to defective condensate formation, caused a reduction in Dvl2-induced luciferase expression (Fig. S5F). The reduced luciferase activity in the presence of the ubiquitin K63R mutant was not due to reduction in Dvl2 protein levels (Fig. S5G) but due to defective condensate formation. Deletion of WWP2 in cells also reduced the Wnt-dependent luciferase activity in cells (Fig. 5D). Furthermore, Wnt3a-induced active β-catenin levels were reduced in WWP2 KO cells compared to those in wild-type cells (Fig. 5E). A similar reduction in active β-catenin was observed in WWP2-depleted cells treated with Wnt3a ligand (Fig. S5H). In addition, Wnt3a-dependent translocation of active β-catenin to the nucleus was not observed in WWP2-depleted cells (Fig. 5F,G). Defective nuclear translocation of β-catenin in WWP2-depleted cells resulted in reduced Wnt-dependent target
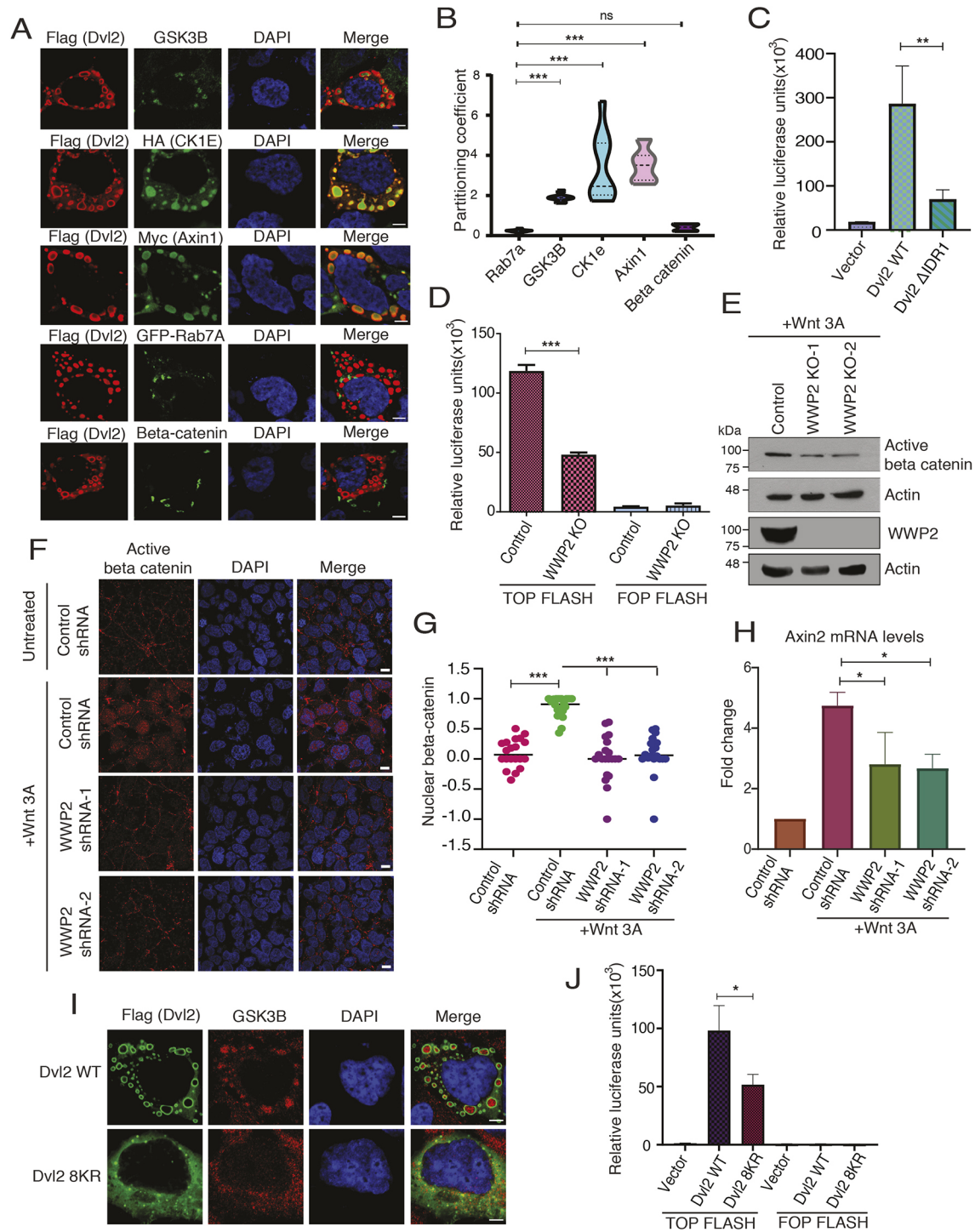
Fig. 5. See next page for legend.

gene expression (Fig. 5H). To further substantiate the role of Dvl2 condensates in activation of the Wnt pathway, we utilized the 8KR version, a condensate-deficient mutant of Dvl2, to test its effect in Wnt signalling. Whereas wild-type Dvl2 could efficiently sequester the component of destruction complex (GSK3β), 8KR mutant was unable to do so (Fig. 5I). Consequently, expression of Dvl2 8KR mutant significantly reduced Wnt-dependent luciferase activity in cells (Fig. 5J). Together, these data suggest that Dvl2 phase separation is important for enhancing Wnt signalling in cells.

DISCUSSION

A remarkable feature of dishevelled family proteins is their ability to form distinct cytoplasmic puncta termed signalosomes. The physiological relevance of the puncta has been always debated, as many studies suggested that they are important in Wnt signalling via regulating destruction complex, whereas others challenge the same idea (Bilić et al., 2007; Schwarz-Romond et al., 2007b; Smalley et al., 2005). Our study here demonstrates that Dvl2 undergoes liquid–liquid phase separation in cells, which is important for relaying the Wnt signal in cells. The phase-separated Dvl2

Fig. 5. Dvl2 phase separation promotes Wnt signalling. (A) Cells were transfected with SFB–DVL2 alone or with HA-tagged CK1ε, Myc-tagged axin 1 or GFP-tagged Rab7a for 24 h. Cells were then fixed and stained with the indicated antibodies and imaged under a confocal microscope. Scale bars: 5 μm. (B) The partitioning coefficient was measured by calculating the ratio of intensity of each protein inside to the intensity outside the condensate and plotted as a violin plot. n=10 cells (10 condensates per each cell). The dashed lines represent the median and interquartile range. ***P<0.001 (one-way ANOVA with Tukey's multiple comparisons test). (C) HEK293T cells were co-transfected with the TCF/LEF reporter plasmid (TOP FLASH) and SFB–Dvl2 WT or ΔIDR mutant. At 24 h post transfection, cells were lysed and luciferase assay was undertaken with a dual luciferase kit (Promega). Values were normalized to *Renilla* luciferase. Error bar indicates s.d., n=2. **P<0.01 (one-way ANOVA with Tukey's multiple comparisons test). (D) Control and WWP2 KO cells were transfected with TOP FLASH or FOP FLASH vectors along with Wnt3a for 24 h. The luciferase assay was undertaken with a dual luciferase kit (Promega). Error bar indicates s.d., n=2. ***P<0.001 (one-way ANOVA with Tukey's multiple comparisons test). (E) Control and WWP2 KO cells were treated with Wnt3a ligand. Cells were lysed in NETN lysis buffer and immunoblotted with non-phosphorylated β-catenin (active β-catenin) antibody and the other indicated antibodies. Blot shown is representative of three independent experiments. (F) Control shRNA- or WWP2 shRNA-treated cells were cultured in serum free medium for 12 h and then treated with Wnt3a (200 ng/ml) for 2 h. Cells were then fixed and stained with with non-phosphorylated β-catenin antibody and imaged using a confocal microscope. Scale bars: 10 μm. (G) Quantification of nuclear with non-phosphorylated β-catenin. Nuclear β-catenin was quantified by measuring the colocalization of β-catenin with DAPI. The line represents the median, n=20 cells. ***P<0.001 (one-way ANOVA with Tukey's multiple comparisons test). (H) Control and WWP2-knockdown cells were cultured in serum free medium for 12 h and treated with Wnt3a (200 ng/ml) for 2 h. *AXIN2* mRNA levels were detected by qRT-PCR. Error bar indicates s.d. *P<0.05 (one-way ANOVA with Tukey's multiple comparisons test). (I) SFB–Dvl2 WT or the 8KR mutant was transfected in HEK293T cells for 24 h. Cells were stained with anti-Flag and anti-GSK3β antibodies and imaged under a microscope. Scale bars: 5 μm. Images in I are representative of three independent experiments. (J) HEK293T cells transfected with either TOP FLASH or FOP FLASH along with SFB–Dvl2 WT or the 8KR mutant for 24 h. Cells were then lysed and luciferase assay was performed using the dual luciferase kit (Promega). Values were normalized to *Renilla* luciferase. Error bar indicates s.d., n=2. *P<0.05 (one-way ANOVA with Tukey's multiple comparisons test).

condensates can accommodate the components of destruction complex and thereby spatially separate the destruction complex and β-catenin. Recently, axin along with APC was also shown to phase separate to recruit destruction complex along with β-catenin and enhance the local concentration of destruction components and control Wnt activation by degrading β-catenin (Li et al., 2020; Nong et al., 2021). Given the functionally opposing roles in regulating β-catenin levels, we believe that Dvl2 condensates are distinct from axin and APC condensates. In fact, in the presence of the Wnt ligand, Dvl2 condensates might be acting one level above axin condensates to recruit all the destruction components including axin condensates to promote Wnt signalling.

Importantly, we identified a critical role for WWP2-mediated ubiquitylation during phase separation of Dvl2. We demonstrated that phase separation of Dvl2 is essential for full activation of Wnt signalling. Multiple E3 ligases, such as ITCH, SMURF1, KLHL12 and NEDD4L, have been identified as regulating Dvl2 ubiquitylation (Angers et al., 2006; Bernatik et al., 2020; Ding et al., 2013; Wei et al., 2012). However, these E3 ligases were shown to inhibit Wnt signalling by promoting Dvl2 degradation. In this study, we identified a non-degradative ubiquitylation of Dvl2 by WWP2 that enhances Wnt signalling. WWP2 has been characterized as an oncogenic E3 ligase in cells, and is known to promote cell survival and proliferation signalling via regulating specific set of tumour

suppressor proteins (Bernassola et al., 2019; Soond and Chantry, 2011). Given that WWP2 has been implicated as a potential oncogene in wide variety of cancers, its limited degradative substrates such as PTEN and p73, might not fully explain the functional repertoire of its oncogenic nature in multiple cancers (Chaudhary and Maddika, 2014; Maddika et al., 2011). Thus, our study identifying Dvl2, a crucial component of Wnt pathway that promotes proliferation and tumour growth, as a new non-degrative substrate might add a new dimension to the oncogenic function of WWP2 in certain cancers. On the other hand, ubiquitylation, as a post-translational modification, has been implicated in numerous cellular functions, such as protein homeostasis, endocytosis and DNA damage signalling, via forming distinct ubiquitin chain linkages (Brinkmann et al., 2015; Haglund and Dikic, 2012; Rape, 2018). Our findings show that there is an important role of a non-canonical K63 linkage in liquid–liquid phase separation of Dvl2.

Ubiquitylation, although being one of the most critical post-translational modifications, has not been studied extensively pertaining to its effect on phase separation of proteins. Exceptions to this are some recent findings showing the role of polyubiquitin chains in eliminating the phase separation behaviour of UBQLN2 (Dao et al., 2018). In another study, ubiquitin-dependent phase separation of proteosome in nucleus was reported (Yasuda et al., 2020). Studies from different groups have shown that K63-linked ubiquitin chains can promote phase separation by providing additional multivalency to proteins like UBQLN2, NEMO (also known as IKBKG) and p62 (Dao et al., 2022; Du et al., 2022; Sun et al., 2018). Interestingly, all these studies depict the regulation of protein phase behaviour by mere interaction with the polyubiquitin chain rather than protein getting covalently modified by ubiquitylation. Our findings clearly demonstrate that K63-linked ubiquitylation on the substrate protein can affect its phase separation. K63 linkage is the second most abundant ubiquitin linkage found in cells. K63 linkage ubiquitylation is largely associated with proteasome-independent functions, such as endocytosis and signal transduction (Husnjak and Dikic, 2012; Komander and Rape, 2012). Recent studies also report that K63 ubiquitylation can trigger proteasomal degradation by seeding branched ubiquitin chains (Ohtake et al., 2018). Our study adds a new regulatory role for K63-linked ubiquitin chains in protein phase separation.

Liquid–liquid phase separation is emerging as a functionally relevant event for many proteins in various cellular contexts. Having different types of ubiquitin linkages available in the cell with only limited functions assigned to them hitherto (Li and Ye, 2008), we speculate that distinct ubiquitin linkages might have an important regulatory role in phase separation of some of these proteins. It would be interesting to test and understand whether different ubiquitin chain topologies have a role in phase separation of other proteins in future studies.

MATERIALS AND METHODS
Plasmids
cDNAs for WWP2 and Dvl2 were purchased from Dharmacon. Axin and CKIε expression plasmids were kind gift from Dr Mariann Bienz (MRC Laboratory of Molecular Biology, Cambridge Biomedical Campus, UK), and V5–Frizzled 5 expression plasmid was a gift from Dr Madelon Maurice (Utrecht University, The Netherlands). All cDNAs were PCR-amplified and cloned into donor vector pDONOR201 (Invitrogen) using gateway cloning and then moved to triple-tagged SFB, Myc, GFP glutathione S-transferase (GST) or MBP-tagged destination vector (Invitrogen) for expression. SFB–Rab5a, SFB–Rab7a and GFP–Rab11 were described in our previous study (Shinde and Maddika, 2016, 2017). All clones were verified by sequencing. All the genes used in the study are of human origin. All the point mutations

and domain deletions {ΔPDZ [deletion of amino acids (aa) 263–352], ΔIDR1 (deletion of aa 94–252) and ΔDEP (deletion of aa 421–502)} were generated by PCR-based site directed mutagenesis and cloned into SFB-, Myc- and GST-tagged expression vectors. ΔDIX (deletion of aa 1–93), ΔCT (deletion of aa 515–736) and CT Dvl2 (aa 515–736) were amplified from full-length Dvl2 and cloned into pDONOR201. To generate DUB–DVL2 fusion proteins, a wild-type and catalytically inactive DUB domain of USP7 was PCR amplified and fused with full-length Dvl2 using overlap PCR. Lentiviral-based shRNAs for WWP2 (shRNA 1 sequence, 5′-ATAAAGCGAAAGTAGGTGAGG-3′; shRNA2 sequence, 5′-TTGAC-GATTATGCACCTTGGG-3′) and UBA1 (shRNA 1 sequence: 5′-ATG-GTGATCTCTAATTTGTGC-3′; shRNA 2 sequence, 5′-TTAACTTCGT-GACATCCCAGG-3′) were purchased from Dharmacon. Lentiviral vectors encoding WWP2 guide RNAs were purchased from transOMIC technologies.

Antibodies
The following antibodies have been used in this study: WWP2 (1:1000; A 302-935A, Bethyl Laboratories), Dvl2 [1:1000 western blotting (WB) and 1:200 immunoprecipitation (IP); 3216S, Cell Signaling Technology, and 1:1000; sc8026, Santa Cruz Biotechnology], non-phospho-β-catenin [1:1000 WB; 1:200 immunofluorescence (IF); 19807S, Cell Signaling Technology], GSK3β (1:200 IF; 12456T, Cell Signaling Technology), Lamp2 (1:200; GL2A7, DSHB), CD63 (1:100; H5C6, DSHB), Flag (1:10,000; F3165, Sigma), actin (1:10,000; A5441, Sigma), Myc (1:1000; sc40, Santa Cruz Biotechnology), ubiquitin (1:2000; 05944, Millipore), and HA (1:2000 WB; 1:200 IF; NB 600-363, Novus Biologicals). V5-tag antibody (1:5000 WB; R 960-25, Thermo Fisher Scientific) was a kind gift from Dr Rashna Bhandari, CDFD, India. HRP-conjugated anti-mouse and anti-rabbit-IgG secondary antibodies were obtained from Jackson Immunologicals.

Cell lines and transfections
HEK293T, U2OS, HepG2, RPE1 and BOSC23 cell lines were used in this study. HEK293T and BOSC23 cells were grown in RPMI (AL028A, HIMEDIA) containing 10% donor bovine serum (DBS; SH30075.03, Hyclone) and 1% penicillin and streptomycin (CC502-0100, GeneDireX). U2OS, HepG2 and RPE1 cells were grown in DMEM (AL007, HIMEDIA) containing 10% fetal bovine serum (FBS; 10270-106, Gibco) and 1% penicillin and streptomycin (CC502-0100, GeneDireX). All cell lines were purchased from American Type Culture Collection, which were tested and authenticated by the cell bank using their standard short tandem repeat (STR)-based techniques. Cells were also continuously monitored by microscopy to ensure that they had maintained their original morphology and also tested for mycoplasma contamination by using DAPI staining. HEK293T and BOSC23 cells were transfected with various plasmids using PEI (Polysciences) according to the manufacturer's protocol. Briefly, the plasmid was diluted in serum-free RPMI medium was mixed with PEI (1 μg/μl) in 1:3 ratios. After incubating the DNA and PEI mixture at room temperature (RT) for 15 min, the complexes were added to cells to allow the transfection of plasmid. Transfections in U2OS, HepG2 and RPE1 cells were done using Turbofect transfection reagent according to the manufacturer's protocol.

Generation of WWP2 and Dvl2 KO cell lines
WWP2 and Dvl2 KO HEK293T cell lines were established using the CRISPR/Cas9 system. In brief, guide RNAs (TEVH-1147610 and TEVH-1080468) targeting WWP2 and non-targeting control (TELA1011) were purchased from transOMIC technologies (pCLIP-All-EFS-Puro vector). gRNA sequence targeting Dvl2 (5′-CTACATTGGCTCCATCATGA-3′) was cloned into Crispr-V2 plasmid for this study. Plasmids were transfected into cells with Turbofect according to the manufacturer's protocol. After 48 h, cells were treated with puromycin (2 μg/ml) and further subjected to clonal selection. Positive clones were verified by western blotting with either WWP2 or Dvl2 antibody for the loss of expression.

Lentiviral infection
Lentivirus-based WWP2 and UBA1 shRNA coding plasmids purchased from Dharmacon were transfected transiently using PEI (Invitrogen) in

BOSC23 packaging cells along with packaging vectors (psPAX2 and pMD2.G; Addgene #12259 and #12260). At 48 h post transfection, the viral medium was collected, filtered through a 0.45 μM filter (9913-2504, Whatman) and added to the target cells along with polybrene (8 μg/ml; H9268, Sigma). At 72 h post infection, cells were collected and processed for various assays and immunoblotting was performed with the specific antibodies to check the efficiency of knockdown.

Tandem affinity purification
Dvl2-associated proteins were isolated by using tandem affinity purification as described previously (Kumar et al., 2017). Briefly, HEK293T cells transiently expressing SFB–Dvl2 were lysed with NETN buffer (20 mM Tris-HCl pH 8.0, 100 mM NaCl, 1 mM EDTA and 0.5% Nonidet P-40) containing 1 μg/ml of each of pepstatin A and aprotinin on ice for 20 min. Lysate was then incubated with streptavidin–Sepharose (Amersham Biosciences) for 2 h at 4°C. After removing the unbound proteins by washing the beads three times with lysis buffer, the associated proteins were eluted using 2 mg/ml biotin (Sigma) for 2 h at 4°C. The eluate was then incubated with S-protein–agarose (Millipore) beads for 1 h at 4°C. After clearing the unbound proteins by washing, the proteins associated with S-protein–agarose beads were eluted by boiling in SDS-loading buffer for 10 min at 95°C. The proteins were identified by mass spectrometry analysis carried out by the Taplin biological mass spectrometry facility at Harvard University.

Immunoprecipitation
For immunoprecipitation assays, cells were lysed with NETN buffer as described above. The whole-cell lysates obtained by centrifugation (16,000 *g* for 10 min) were incubated with 2 μg of specified antibody bound to either protein A or protein G–sepharose beads or with streptavidin–sepharose beads (Amersham Biosciences) for 1 h at 4°C. The immunocomplexes were then washed with NETN buffer three times and subjected to SDS-PAGE. Immunoblotting was performed using standard protocols.

Immunofluorescence
Cells grown on coverslips were fixed with 3% paraformaldehyde for 15 min at room temperature and permeabilized with 0.2% Triton X-100 for 5 min at room temperature. For staining with Dvl2 antibody, cells were fixed with 4% paraformaldehyde for 15 min at room temperature and permeabilized with ice-cold methanol at −20°C for 10 min. Permeabilized cells were then incubated with a 5% BSA for blocking at RT for 60 min followed by incubation with primary antibodies for 60 min at room temperature. After incubation, cells were washed three times with 1× PBS and then incubated with FITC- or Rhodamine-conjugated secondary antibodies at RT for 60 min followed by three washes with 1× PBS. Nuclei were counterstained with DAPI. Cells were washed with PBS, and coverslips were mounted with glycerol containing paraphenylenediamine and imaged using a confocal microscope (LSM, 700 Zeiss). We used maximum intensity projection for all the quantifications but for representative images for the figures, we used images from particular focal plane.

Recombinant protein purification
GST- and MBP-tagged full-length Dvl2 and WWP2 were transformed into *Escherichia coli* BL21 (DE3) cells. Cultures were grown to an optical density (OD) at 600 nm of ∼0.6 and induced with 0.5 mM isopropyl β-D-1-thiogalactopyranoside (IPTG) at 37°C for 4 h. For MBP, WWP2 the cell pellet (18,000 *g* for 20 min) was lysed in lysis buffer [50 mM Tris-HCl pH 7.5, 150 mM NaCl, and 0.01% NP–40 Igepal and protease inhibitors (Aprotinin, A1153, Sigma; Pepstatin, 9000469, Cayman Chemicals; PMSF, 78830, Sigma)] and sonicated. Cell lysates were pulled down with dextran–Sepharose beads (28-9355-97, GE Heathcare) for 2 h at 4°C. Then, beads were washed five times with wash buffer (50 mM Tris-HCl pH 7.5, 300 mM NaCl, 0.01% NP–40 Igepal, 1 mM DTT and protease inhibitors) and bound proteins were eluted with the elution buffer containing 20 mM Tris-HCl pH 7.5, 200 mM NaCl, 1 mM EDTA and 10 mM maltose. For GST, the Dvl2 cell pellet was lysed in lysis buffer (50 mM Tris-HCl pH 8, 500 mM NaCl, 1 mM EDTA and 1.5% sarkosyl).

GST–Dvl2 was eluted with elution buffer containing 50 mM Tris-HCl pH 8, 500 mM NaCl, 100 mM reduced glutathione.

Ubiquitylation assay

In vitro ubiquitylation assays were carried out at 30°C for 15 min in 25 µl of ubiquitylation reaction buffer [50 mM Tris-HCl pH 7.6, 2 mM dithiothreitol (DTT), 5 mM MgCl$_2$, 0.1 M NaCl and 2 mM ATP] containing the following components: 100 µM ubiquitin, 20 nM E1 (UBE1) and 100 nM UbcH7 (all from Boston Biochem), 1 µg bacterially purified MBP–WWP2 WT or catalytically dead mutant (with a C838A mutation) was added to the reaction mixture. Bacterially purified GST–Dvl2 bound to glutathione–Sepharose beads (Amersham) were used as substrates in the reaction mixture. After the reaction, beads were washed three times with wash buffer (50 mM Tris-HCL pH 7.5, 300 mM NaCl, 0.05% NP-40 and 1 mM DTT) and boiled with SDS-PAGE loading buffer; ubiquitylation of substrates was detected by western blotting with anti-ubiquitin antibody. For *in vivo* ubiquitylation assays, at 24 h post transfection with the indicated plasmids, cells were harvested and lysed under denaturing condition (50 mM Tris-HCl pH 7.5, 100 mM β-mercaptoethanol, 1% SDS and 5 mM EDTA). Lysate was subjected to streptavidin–Sepharose-mediated pulldown and ubiquitylation was detected by immunoblotting with ubiquitin or Flag antibody.

In vitro droplet assay

GST Dvl2 eluted in high salt-containing elution buffer (50 mM Tris-HCl pH 8, 500 mM NaCl, 100 mM reduced glutathione) was mixed with phase-separation buffer (25 mM Tris-HCl pH 7.4, 100 mM KCl, 2.5% glycerol, 0.5 mM DTT) to get a final salt concentration of 150 mM. 10 µl of GST–Dvl2 in phase separation buffer was mounted as a drop on slide and the droplets formed were imaged under a bright field microscope.

Luciferase assay

HEK293T cells were transfected with either with TOP Flash or FOP Flash reporter plasmids and *Renilla* luciferase plasmid and other indicated plasmids. At 24 h post transfection, cells were lysed and the assay was performed with a dual luciferase kit (Promega) according to the manufacturer's protocol. Values were normalized to those of *Renilla* luciferase.

FRAP assay

GFP–Dvl2 condensates were selectively bleached with 488 nm argon laser (Zeiss LSM 700 confocal microscope). Recovery was monitored by acquisition of images for the following 4 min at 10 s intervals at room temperature. Fluorescence intensity of unbleached condensates from the same cells were also monitored.

Cycloheximide-chase assay

Cells transfected with empty vector or Myc–WWP2 WT for 24 h were then treated with cycloheximide (50 µg/ml; C7698, Sigma). Cells were harvested at different time points and protein levels were detected by immunoblotting.

1,6-hexanediol treatment

Cells grown in glass bottom dishes were transfected with GFP–Dvl2. After 24 h of transfection, cells were treated with 3% hexanediol (7046, TOCRIS) and were imaged for 4 min by acquiring images at every 3 s under the Leica DMi8 live-cell imaging platform. Cells were maintained at 37°C and 90% humidity throughout the imaging. Untreated cells were imaged as control.

Quantitative real-time PCR

Control and WWP2 knockdown cells were cultured in serum free medium for 12 h followed by the addition of 200 ng/ml of recombinant Wnt3a for 2 h. Cells were then lysed and RNA was isolated using Nucleospin RNA isolation kit (MACHERY-NAGEL) following the manufacturer's protocol. 1 µg of total RNA was used to synthesize cDNA using Takara cDNA synthesis kit. qRT-PCR was performed using the TB Green Premix Ex TaqII (Tli RNaseH plus) kit (Takara Bio) in a Bio real-time PCR system as per manufacturer's protocol. The primer sequences used to amplify axin is were: axin 2 forward primer-5′-GTGAGGTCCACGGAAACTGT-3′; axin 2 reverse primer, 5′-GTGGGTTCTCGGGAAATGA-3′.

References

Aberle, H., Bauer, A., Stappert, J., Kispert, A. and Kemler, R. (1997). β-catenin is a target for the ubiquitin-proteasome pathway. *EMBO J.* **16**, 3797-3804. doi:10.1093/emboj/16.13.3797

Angers, S., Thorpe, C. J., Biechele, T. L., Goldenberg, S. J., Zheng, N., Maccoss, M. J. and Moon, R. T. (2006). The KLHL12-Cullin-3 ubiquitin ligase negatively regulates the Wnt-beta-catenin pathway by targeting Dishevelled for degradation. *Nat. Cell Biol.* **8**, 348-357. doi:10.1038/ncb1381

Behrens, J., Von Kries, J. P., Kühl, M., Bruhn, L., Wedlich, D., Grosschedl, R. and Birchmeier, W. (1996). Functional interaction of beta-catenin with the transcription factor LEF-1. *Nature* **382**, 638-642. doi:10.1038/382638a0

Bernassola, F., Chillemi, G. and Melino, G. (2019). HECT-type E3 ubiquitin ligases in cancer. *Trends Biochem. Sci.* **44**, 1057-1075. doi:10.1016/j.tibs.2019.08.004

Bernatik, O., Paclikova, P., Sri Ganji, R. and Bryja, V. (2020). Activity of Smurf2 ubiquitin ligase is regulated by the Wnt pathway protein dishevelled. *Cells* **9**, 1147. doi:10.3390/cells9051147

Bilić, J., Huang, Y.-L., Davidson, G., Zimmermann, T., Cruciat, C.-M., Bienz, M. and Niehrs, C. (2007). Wnt induces LRP6 signalosomes and promotes dishevelled-dependent LRP6 phosphorylation. *Science* **316**, 1619-1622. doi:10.1126/science.1137065

Boeynaems, S., Alberti, S., Fawzi, N. L., Mittag, T., Polymenidou, M., Rousseau, F., Schymkowitz, J., Shorter, J., Wolozin, B., Van Den Bosch, L. et al. (2018). Protein phase separation: a new phase in cell biology. *Trends Cell Biol.* **28**, 420-435. doi:10.1016/j.tcb.2018.02.004

Brinkmann, K., Schell, M., Hoppe, T. and Kashkar, H. (2015). Regulation of the DNA damage response by ubiquitin conjugation. *Front. Genet.* **6**, 98. doi:10.3389/fgene.2015.00098

Chaudhary, N. and Maddika, S. (2014). WWP2-WWP1 ubiquitin ligase complex coordinated by PPM1G maintains the balance between cellular p73 and DeltaNp73 levels. *Mol. Cell. Biol.* **34**, 3754-3764. doi:10.1128/MCB.00101-14

Clevers, H. (2006). Wnt/beta-catenin signaling in development and disease. *Cell* **127**, 469-480. doi:10.1016/j.cell.2006.10.018

Cong, F., Schweizer, L. and Varmus, H. (2004). Wnt signals across the plasma membrane to activate the β-catenin pathway by forming oligomers containing its receptors, Frizzled and LRP. *Development* **131**, 5103-5115. doi:10.1242/dev.01318

Dao, T. P., Kolaitis, R.-M., Kim, H. J., O'donovan, K., Martyniak, B., Colicino, E., Hehnly, H., Taylor, J. P. and Castañeda, C. A. (2018). Ubiquitin modulates liquid-liquid phase separation of UBQLN2 via disruption of multivalent interactions. *Mol. Cell* **69**, 965-978.e6. doi:10.1016/j.molcel.2018.02.004

Dao, T. P., Yang, Y., Presti, M. F., Cosgrove, M. S., Hopkins, J. B., Ma, W., Loh, S. N. and Castaneda, C. A. (2022). Mechanistic insights into enhancement or inhibition of phase separation by different polyubiquitin chains. *EMBO Rep.* **23**, e55056. doi:10.15252/embr.202255056

Ding, Y., Zhang, Y., Xu, C., Tao, Q.-H. and Chen, Y.-G. (2013). HECT domain-containing E3 ubiquitin ligase NEDD4L negatively regulates Wnt signaling by targeting dishevelled for proteasomal degradation. *J. Biol. Chem.* **288**, 8289-8298. doi:10.1074/jbc.M112.433185

Du, M., Ea, C.-K., Fang, Y. and Chen, Z. J. (2022). Liquid phase separation of NEMO induced by polyubiquitin chains activates NF-kappaB. *Mol. Cell* **82**, 2415-2426.e5. doi:10.1016/j.molcel.2022.03.037

Elbaum-Garfinkle, S. (2019). Matter over mind: Liquid phase separation and neurodegeneration. *J. Biol. Chem.* **294**, 7160-7168. doi: 10.1074/jbc.REV118.001188

Fiedler, M., Mendoza-Topaz, C., Rutherford, T. J., Mieszczanek, J. and Bienz, M. (2011). Dishevelled interacts with the DIX domain polymerization interface of Axin to interfere with its function in down-regulating β-catenin. *Proc. Natl. Acad. Sci. USA* **108**, 1937-1942. doi:10.1073/pnas.1017063108

Gammons, M. V., Renko, M., Johnson, C. M., Rutherford, T. J. and Bienz, M. (2016a). Wnt signalosome assembly by DEP domain swapping of dishevelled. *Mol. Cell* **64**, 92-104. doi:10.1016/j.molcel.2016.08.026

Gammons, M. V., Rutherford, T. J., Steinhart, Z., Angers, S. and Bienz, M. (2016b). Essential role of the Dishevelled DEP domain in a Wnt-dependent human-cell-based complementation assay. *J. Cell Sci.* **129**, 3892-3902. doi:10.1242/jcs.195685

Gao, C. and Chen, Y.-G. (2010). Dishevelled: the hub of Wnt signaling. *Cell. Signal.* **22**, 717-727. doi:10.1016/j.cellsig.2009.11.021

Haglund, K. and Dikic, I. (2012). The role of ubiquitylation in receptor endocytosis and endosomal sorting. *J. Cell Sci.* **125**, 265-275. doi:10.1242/jcs.091280

Harnoš, J., Cañizal, M. C. A., Jurásek, M., Kumar, J., Holler, C., Schambony, A., Hanáková, K., Bernatík, O., Zdráhal, Z., Gömöryová, K. et al. (2019). Dishevelled-3 conformation dynamics analyzed by FRET-based biosensors reveals a key role of casein kinase 1. *Nat. Commun.* **10**, 1804. doi:10.1038/s41467-019-09651-7

Hawkins, N. C., Ellis, G. C., Bowerman, B. and Garriga, G. (2005). MOM-5 frizzled regulates the distribution of DSH-2 to control C. elegans asymmetric neuroblast divisions. *Dev. Biol.* **284**, 246-259. doi:10.1016/j.ydbio.2005.05.024

Husnjak, K. and Dikic, I. (2012). Ubiquitin-binding proteins: decoders of ubiquitin-mediated cellular functions. *Annu. Rev. Biochem.* **81**, 291-322. doi:10.1146/annurev-biochem-051810-094654

Kan, W., Enos, M. D., Korkmazhan, E., Muennich, S., Chen, D.-H., Gammons, M. V., Vasishtha, M., Bienz, M., Dunn, A. R., Skiniotis, G. et al. (2020). Limited dishevelled/Axin oligomerization determines efficiency of Wnt/β-catenin signal transduction. *eLife* **9**, e55015. doi:10.7554/eLife.55015

Kishida, S., Yamamoto, H., Hino, S., Ikeda, S., Kishida, M. and Kikuchi, A. (1999). DIX domains of Dvl and axin are necessary for protein interactions and their ability to regulate β-catenin stability. *Mol. Cell. Biol.* **19**, 4414-4422. doi:10.1128/MCB.19.6.4414

Komander, D. and Rape, M. (2012). The ubiquitin code. *Annu. Rev. Biochem.* **81**, 203-229. doi:10.1146/annurev-biochem-060310-170328

Kumar, P., Munnangi, P., Chowdary, K. R., Shah, V. J., Shinde, S. R., Kolli, N. R., Halehalli, R. R., Nagarajaram, H. A. and Maddika, S. (2017). A human tyrosine phosphatase interactome mapped by proteomic profiling. *J. Proteome Res.* **16**, 2789-2801. doi:10.1021/acs.jproteome.7b00065

Lee, Y.-N., Gao, Y. and Wang, H.-Y. (2008). Differential mediation of the Wnt canonical pathway by mammalian Dishevelleds-1, -2, and -3. *Cell. Signal.* **20**, 443-452. doi:10.1016/j.cellsig.2007.11.005

Lee, H.-J., Shi, D.-L. and Zheng, J. J. (2015). Conformational change of Dishevelled plays a key regulatory role in the Wnt signaling pathways. *eLife* **4**, e08142. doi:10.7554/eLife.08142

Li, W. and Ye, Y. (2008). Polyubiquitin chains: functions, structures, and mechanisms. *Cell. Mol. Life Sci.* **65**, 2397-2406. doi:10.1007/s00018-008-8090-6

Li, H., Zhang, Z., Wang, B., Zhang, J., Zhao, Y. and Jin, Y. (2007). Wwp2-mediated ubiquitination of the RNA polymerase II large subunit in mouse embryonic pluripotent stem cells. *Mol. Cell. Biol.* **27**, 5296-5305. doi:10.1128/MCB.01667-06

Li, T.-M., Ren, J., Husmann, D., Coan, J. P., Gozani, O. and Chua, K. F. (2020). Multivalent tumor suppressor adenomatous polyposis coli promotes Axin biomolecular condensate formation and efficient β-catenin degradation. *Sci. Rep.* **10**, 17425. doi:10.1038/s41598-020-74080-2

Lv, Y., Zhang, K. and Gao, H. (2014). Paip1, an effective stimulator of translation initiation, is targeted by WWP2 for ubiquitination and degradation. *Mol. Cell. Biol.* **34**, 4513-4522. doi:10.1128/MCB.00524-14

Ma, W., Chen, M., Kang, H., Steinhart, Z., Angers, S., He, X. and Kirschner, M. W. (2020). Single-molecule dynamics of Dishevelled at the plasma membrane and Wnt pathway activation. *Proc. Natl. Acad. Sci. USA* **117**, 16690-16701. doi:10.1073/pnas.1910547117

Maddika, S., Kavela, S., Rani, N., Palicharla, V. R., Pokorny, J. L., Sarkaria, J. N. and Chen, J. (2011). WWP2 is an E3 ubiquitin ligase for PTEN. *Nat. Cell Biol.* **13**, 728-733. doi:10.1038/ncb2240

Miller, J. R., Rowning, B. A., Larabell, C. A., Yang-Snyder, J. A., Bates, R. L. and Moon, R. T. (1999). Establishment of the dorsal-ventral axis in Xenopus embryos coincides with the dorsal enrichment of dishevelled that is dependent on cortical rotation. *J. Cell Biol.* **146**, 427-437. doi:10.1083/jcb.146.2.427

Molenaar, M., Van De Wetering, M., Oosterwegel, M., Peterson-Maduro, J., Godsave, S., Korinek, V., Roose, J., Destrée, O. and Clevers, H. (1996). XTcf-3 transcription factor mediates beta-catenin-induced axis formation in Xenopus embryos. *Cell* **86**, 391-399. doi:10.1016/S0092-8674(00)80112-9

Molliex, A., Temirov, J., Lee, J., Coughlin, M., Kanagaraj, A. P., Kim, H. J., Mittag, T. and Taylor, J. P. (2015). Phase separation by low complexity domains promotes stress granule assembly and drives pathological fibrillization. *Cell* **163**, 123-133. doi:10.1016/j.cell.2015.09.015

Moriguchi, T., Kawachi, K., Kamakura, S., Masuyama, N., Yamanaka, H., Matsumoto, K., Kikuchi, A. and Nishida, E. (1999). Distinct domains of mouse dishevelled are responsible for the c-Jun N-terminal kinase/stress-activated protein kinase activation and the axis formation in vertebrates. *J. Biol. Chem.* **274**, 30957-30962. doi:10.1074/jbc.274.43.30957

Mund, T., Graeb, M., Mieszczanek, J., Gammons, M., Pelham, H. R. B. and Bienz, M. (2015). Disinhibition of the HECT E3 ubiquitin ligase WWP2 by polymerized Dishevelled. *Open Biol.* **5**, 150185. doi:10.1098/rsob.150185

Nong, J., Kang, K., Shi, Q., Zhu, X., Tao, Q. and Chen, Y.-G. (2021). Phase separation of Axin organizes the β-catenin destruction complex. *J. Cell Biol.* **220**, e202012112. doi:10.1083/jcb.202012112

Ohtake, F., Tsuchiya, H., Saeki, Y. and Tanaka, K. (2018). K63 ubiquitylation triggers proteasomal degradation by seeding branched ubiquitin chains. *Proc. Natl. Acad. Sci. USA* **115**, E1401-E1408. doi:10.1073/pnas.1716673115

Qi, J., Lee, H.-J., Saquet, A., Cheng, X.-N., Shao, M., Zheng, J. J. and Shi, D.-L. (2017). Autoinhibition of Dishevelled protein regulated by its extreme C terminus plays a distinct role in Wnt/β-catenin and Wnt/planar cell polarity (PCP) signaling pathways. *J. Biol. Chem.* **292**, 5898-5908. doi:10.1074/jbc.M116.772509

Rape, M. (2018). Ubiquitylation at the crossroads of development and disease. *Nat. Rev. Mol. Cell Biol.* **19**, 59-70. doi:10.1038/nrm.2017.83

Ribbeck, K. and Gorlich, D. (2002). The permeability barrier of nuclear pore complexes appears to operate via hydrophobic exclusion. *EMBO J* **21**, 2664-71.

Schwarz-Romond, T., Merrifield, C., Nichols, B. J. and Bienz, M. (2005). The Wnt signalling effector Dishevelled forms dynamic protein assemblies rather than stable associations with cytoplasmic vesicles. *J. Cell Sci.* **118**, 5269-5277. doi:10.1242/jcs.02646

Schwarz-Romond, T., Fiedler, M., Shibata, N., Butler, P. J. G., Kikuchi, A., Higuchi, Y. and Bienz, M. (2007a). The DIX domain of Dishevelled confers Wnt signaling by dynamic polymerization. *Nat. Struct. Mol. Biol.* **14**, 484-492. doi:10.1038/nsmb1247

Schwarz-Romond, T., Metcalfe, C. and Bienz, M. (2007b). Dynamic recruitment of axin by Dishevelled protein assemblies. *J. Cell Sci.* **120**, 2402-2412. doi:10.1242/jcs.002956

Shinde, S. R. and Maddika, S. (2016). PTEN modulates EGFR late endocytic trafficking and degradation by dephosphorylating Rab7. *Nat. Commun.* **7**, 10689. doi:10.1038/ncomms10689

Shinde, S. R. and Maddika, S. (2017). PTEN regulates glucose transporter recycling by impairing SNX27 retromer assembly. *Cell Rep.* **21**, 1655-1666. doi:10.1016/j.celrep.2017.10.053

Smalley, M. J., Signoret, N., Robertson, D., Tilley, A., Hann, A., Ewan, K., Ding, Y., Paterson, H. and Dale, T. C. (2005). Dishevelled (Dvl-2) activates canonical Wnt signalling in the absence of cytoplasmic puncta. *J. Cell Sci.* **118**, 5279-5289. doi:10.1242/jcs.02647

Soond, S. M. and Chantry, A. (2011). Selective targeting of activating and inhibitory Smads by distinct WWP2 ubiquitin ligase isoforms differentially modulates TGFβ signalling and EMT. *Oncogene* **30**, 2451-2462. doi:10.1038/onc.2010.617

Stamos, J. L. and Weis, W. I. (2013). The β-catenin destruction complex. *Cold Spring Harb. Perspect. Biol.* **5**, a007898. doi:10.1101/cshperspect.a007898

Sun, D., Wu, R., Zheng, J., Li, P. and Yu, L. (2018). Polyubiquitin chain-induced p62 phase separation drives autophagic cargo segregation. *Cell Res.* **28**, 405-415. doi:10.1038/s41422-018-0017-7

Tauriello, D. V. F., Haegebarth, A., Kuper, I., Edelmann, M. J., Henraat, M., Canninga-Van Dijk, M. R., Kessler, B. M., Clevers, H. and Maurice, M. M. (2010). Loss of the tumor suppressor CYLD enhances Wnt/β-catenin signaling through K63-linked ubiquitination of Dvl. *Mol. Cell* **37**, 607-619. doi:10.1016/j.molcel.2010.01.035

Tauriello, D. V. F., Jordens, I., Kirchner, K., Slootstra, J. W., Kruitwagen, T., Bouwman, B. A. M., Noutsou, M., Rüdiger, S. G. D., Schwamborn, K., Schambony, A. et al. (2012). Wnt/beta-catenin signaling requires interaction of the Dishevelled DEP domain and C terminus with a discontinuous motif in Frizzled. *Proc. Natl. Acad. Sci. USA* **109**, E812-E820. doi:10.1073/pnas.1114802109

Teo, R., Möhrlen, F., Plickert, G., Müller, W. A. and Frank, U. (2006). An evolutionary conserved role of Wnt signaling in stem cell fate decision. *Dev. Biol.* **289**, 91-99. doi:10.1016/j.ydbio.2005.10.009

Torres, M. A. and Nelson, W. J. (2000). Colocalization and redistribution of dishevelled and actin during Wnt-induced mesenchymal morphogenesis. *J. Cell Biol.* **149**, 1433-1442. doi:10.1083/jcb.149.7.1433

Wegmann, S., Eftekharzadeh, B., Tepper, K., Zoltowska, K. M., Bennett, R. E., Dujardin, S., Laskowski, P. R., MacKenzie, D., Kamath, T., Commins, C. et al. (2018). Tau protein liquid-liquid phase separation can initiate tau aggregation. *EMBO J.* **37**, e98049. doi:10.15252/embj.201798049

Wei, W., Li, M., Wang, J., Nie, F. and Li, L. (2012). The E3 ubiquitin ligase ITCH negatively regulates canonical Wnt signaling by targeting dishevelled protein. *Mol. Cell. Biol.* **32**, 3903-3912. doi:10.1128/MCB.00251-12

Xu, H. M., Liao, B., Zhang, Q. J., Wang, B. B., Li, H., Zhong, X. M., Sheng, H. Z., Zhao, Y. X., Zhao, Y. M. and Jin, Y. (2004). Wwp2, an E3 ubiquitin ligase that targets transcription factor Oct-4 for ubiquitination. *J. Biol. Chem.* **279**, 23495-23503. doi:10.1074/jbc.M400516200

Yanagawa, S., Van Leeuwen, F., Wodarz, A., Klingensmith, J. and Nusse, R. (1995). The dishevelled protein is modified by wingless signaling in Drosophila. *Genes Dev.* **9**, 1087-1097. doi:10.1101/gad.9.9.1087

Yasuda, S., Tsuchiya, H., Kaiho, A., Guo, Q., Ikeuchi, K., Endo, A., Arai, N., Ohtake, F., Murata, S., Inada, T. et al. (2020). Stress- and ubiquitylation-dependent phase separation of the proteasome. *Nature* **578**, 296-300. doi:10.1038/s41586-020-1982-9

Yu, A., Rual, J.-F., Tamai, K., Harada, Y., Vidal, M., He, X. and Kirchhausen, T. (2007). Association of Dishevelled with the clathrin AP-2 adaptor is required for Frizzled endocytosis and planar cell polarity signaling. *Dev. Cell* **12**, 129-141. doi:10.1016/j.devcel.2006.10.015